

Photostability of laser dyes incorporated in formamide SiO₂ ORMOSILs

Guadalupe Valverde-Aguilar *

Department of Chemistry and Biochemistry, University of California, Los Angeles, CA 90095, United States

Received 19 April 2005; accepted 11 June 2005

Available online 26 September 2005

Abstract

The sol–gel process provides a low temperature chemical route for the preparation of rigid transparent matrix materials. Under this process, luminescent organic dye molecules were incorporated into organically modified silicate (ORMOSIL) host matrices. The photostability of these laser dyes encapsulated in a solid matrix was studied using optical absorption and luminescence. The photochemical mechanisms of the dye response under N₂ laser irradiation were studied using UV and fluorescence spectra measurement. The evolution of the maximum of the emission and excitation curves as function of accumulated irradiated energy was fitted by exponential equations. The matrix protects the dye from the oxidation and dimerization reactions. The dye molecules exhibited photobleaching due to their photodegradation. The ORMOSIL doped with Nile blue exhibits good photostability after 6 h of irradiation.

© 2005 Elsevier B.V. All rights reserved.

PACS: 42.55.Mv; 81.20.Fw; 32.50.+d; 72.80.Tm

Keywords: ORMOSILs; Photostabilities; Dye laser; Photobleaching

1. Introduction

The sol–gel process has the possibility of improving optical and mechanical properties of materials [1]. In glasses, many elements can be incorporated as inorganic network formers (e.g. SiO₂, ZrO₂, and TiO₂) and as network modifiers (e.g. Na₂O, MgO, BaO). While on the other hand organic network formers such as polymer chains of many types and length (e.g. with aromatic and aliphatic monomer units) and organic network modifiers (e.g. Si–CH₃, Si–C₆H₅) are also possible [2]. Various sol–gel methods have been developed to produce novel glass composite materials [3]. These include organically modified silicates (ORMOSILs). The ORMOSIL is a mixture of an organic component and the inorganic precursor; it combines optical transparency from silica gels with elasticity from polymers. This kind of materials offers some advantages in

comparison to pure inorganic sol–gels because of its superior film formability, allowing thick film to be coated onto glass substrate. In addition, the ORMOSIL matrix has good transparency and is less susceptible to cracking than the pure inorganic sol–gel [4]. This matrix enhances the photostability from laser dyes and they have excellent optical and mechanical properties. For these reasons, the ORMOSILs are a very promising solid-state host medium for organic molecules.

Fluorescent laser dyes have been used for many years as a versatile source of tunable coherent optical radiation; dyes are commonly used in both lasers and optical pumped amplifiers [5–7]. These dyes have been doped into several kinds of solid-state media such as polymer, copolymer, epoxy, polycom, silica glass and ORMOSILs [8]. The main problems that remain are the damage threshold of host materials and photostability of laser dyes, in other words, the longevity of dye-doped samples. The lack of photostability has been the major factor that has limited the commercial use of dye lasers. Photostability of a sample

* Tel.: +1 310 8258651; fax: +1 310 2064038.

E-mail address: valverde@chem.ucla.edu

depends not only on the laser dye and the host composition and structure, but also on factors such as the dye concentration, pump wavelength, pulse rate, pump fluorescence sample, sample thickness, and geometry [9]. Other effect can be detected, the photochemical bleaching of dyes by light. The bleaching of the fluorescent output upon optical pumping, typically reflects the chemical modification of the dye molecule. The bleaching process depends on the nature of the solvent or matrix and the presence of the other reactive impurities such as oxygen [10,11].

In a solid host, the photodegradation of the laser dye depends on the nature of the dye molecule, the composition and structure of the host, and the impurities presented in the host. Two major photochemical reactions, oxidation and dimerization, bring about the destruction of the original dye molecules and permanent drop in the fluorescence output [12]. Intermolecular interactions can also produce photochemical reactions, deactivation processes, and quenching processes. The improved photostability of the dye within solid hosts has been attributed to caging and immobilizing the dye molecules that reduces the interaction with other species (e.g. oxygen, other dyes molecules and impurities) achieving the improvement in photostability with respect to solvent hosts [13,14]. This should reduce the dynamic interactions that can produce degradation.

The dye molecules are introduced into the silica network during the hydrolysis–condensation reaction and the microenvironment where they exist largely depends on the chemical and size compatibility between the dye molecules and the host medium. The chemical compatibility between the dye molecule and the host medium defines that a polar dye molecule prefers to exist in a larger pore where exists residual polar groups, while a nonpolar dye molecule prefer to exist in the nonpolar cage. It is known that covalently bonding the dye into the silica network may increase dye caging and reduce dye aggregation. Also, a more condensed microstructure with smaller pore can sharply decrease the local thermal accumulation and optical loss, in other words, it has a higher homogeneity and thermal conductivity, and limits the mobility of the laser dye molecules, which sharply decreases the possibility of the photochemical reactions between the dyes molecules and other impurities.

The objective of the present work was the synthesis of transparent, crack-free ORMOSILs doped with Nile blue or Rhodamine 6G dyes. We study the photostability of these dye molecules, incorporated into the ORMOSIL matrix by the sol–gel route, as function of host composition. A bleaching effect of the dye molecules was followed as function of the recovery time of the sample, which was kept in the darkness. Our results were compared with those from silica gels doped with Rhodamine 6G.

2. Experimental

The sol was obtained from hydrolysis and polycondensation of tetramethoxysilane (TMOS), using DI-water, with methanol as solvent. Formamide was also being used in the initial reaction to ensure monolithicity of the resulting gels. The molar ratio used of TMOS:water:nitric acid:methanol:formamide was [1:10:0.45:3:3] and the initial volume was 25 ml.

Water/nitric acid mixture was added to the TMOS/methanol/formamide, under magnetic stirring in an open glass beaker. After 30 min of mixing, the dye was added using a concentration of 1.1×10^{-3} M. The molecular structure of the Nile blue 610 and Rhodamine 6G (590) dyes are shown in Fig. 1.

One month after gelation, the containers were opened and the pore liquid expelled during shrinkage and evacuation. Drying and aging were continued at room temperature. Finally, we got transparent orange (R6G) and blue (NB) color samples, but the samples have a paste texture. The sample was cut to a 5×7 mm section. After, it was exposed under N_2 laser using the following time periods: 0.5 h, 2 h, 4 h and 6 h. For each exposure the absorption, emission and excitation spectra were measured to register the evolution of the maximum.

The optical absorption was measured with a Milton Roy 3000 Array Spectrophotometer with a resolution of 2 nm. To determinate the photoluminescence spectral a Luminescence Spectrometer Perkin Elmer Model LS55 was used, it has a 20 kW Xenon discharge lamp with pulse width at half height $<10 \mu\text{s}$; two monochromators, which operate between 220 nm and 900 nm with an accuracy of ± 1 nm and wavelength reproducibility of ± 0.5 nm (Fig. 2).

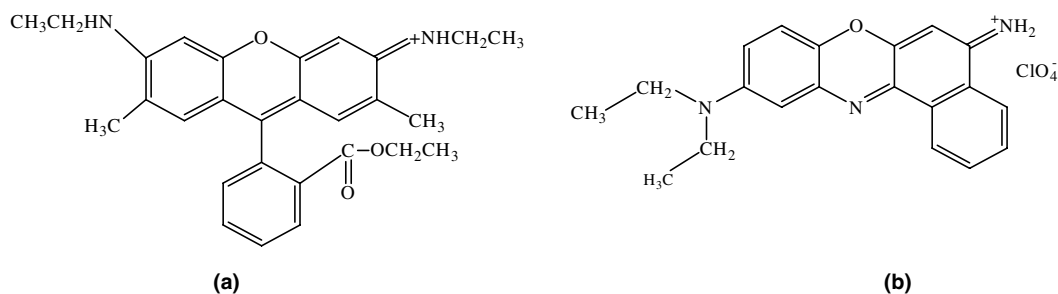


Fig. 1. Molecular structure of dyes. (a) Rhodamine 6G (590) and (b) Nile blue 610.

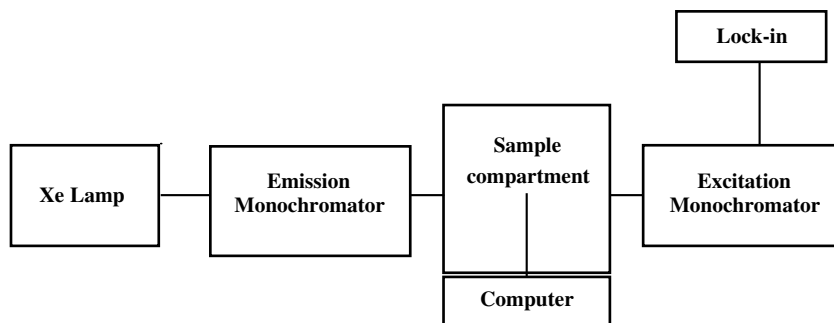


Fig. 2. Scheme of the fluorometer to measure the emission and excitation.

The ORMOSIL samples were irradiated with a Oriel N₂ laser at a frequency of 3.3 pulses/s with a peak power of 80 kW.

3. Results

Our results will be divided in two sections, one corresponding to the R6G ORMOSIL, and the second section corresponding to the NB ORMOSIL.

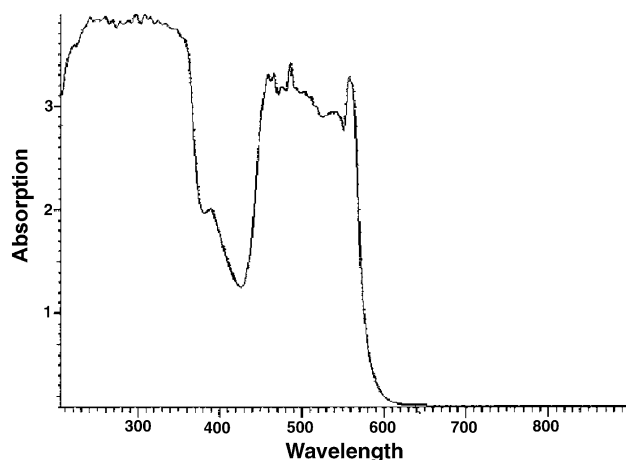


Fig. 3. Absorption spectrum of rhodamine 6G ORMOSIL.

3.1. Rhodamine 6G ORMOSIL

Fig. 3 shows the absorption spectrum of the R6G ORMOSIL, a broad band centered at 530 nm was observed.

Fig. 4(a) shows the emission intensity as function of accumulated irradiated energy. The experimental decay was fitted with equation $Y = Y_0 + e^{-x/t_1}$ (dashed line). When R6G ORMOSIL was irradiated, the amount of deposited energy increased, which caused that the emission decreased exponentially. An opposite behavior is observed in Fig. 4(b), it shows the excitation intensity as function of accumulated irradiated energy. The excitation signal increases until it reaches a maximum value, then it decreases rapidly. The experimental curve was fitted with equation $Y = Y_0 + e^{-(x-c)^2/t_1}$ (dashed line).

The R6G ORMOSIL exhibits a photobleaching effect after 6 h of irradiation and it remained colorless. Then, the sample was kept in the darkness to avoid the sunlight, and the ORMOSIL photoluminescence was followed at different times to detect any change of the sample. Fig. 5 shows the luminescence evolution taking into account the emission intensity of the sample as function of the time. A little recovery was observed at time of 8 h, but the signal decreased for a long time. The R6G ORMOSIL did not regain its color again.

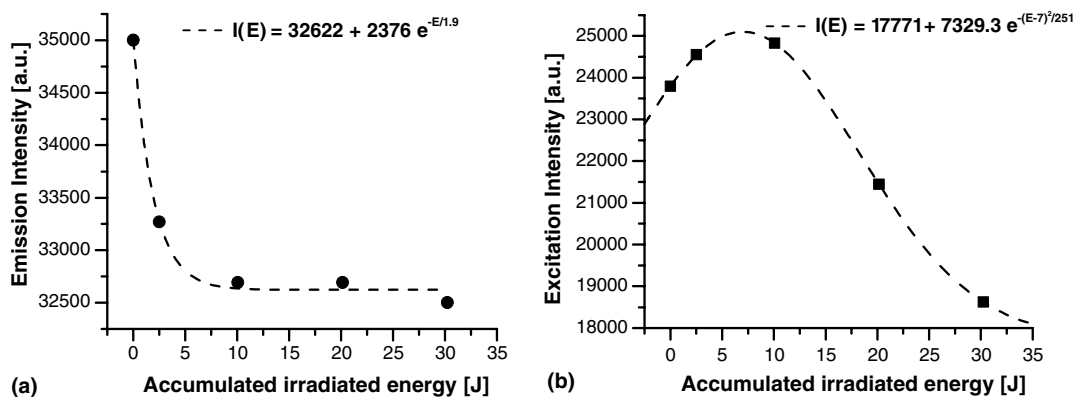


Fig. 4. (a) Emission intensity of R6G ORMOSIL as a function of accumulated irradiated energy with $\lambda_{\text{exc}} = 530$ nm. (b) Excitation intensity of R6G ORMOSIL as a function of accumulated irradiated energy with $\lambda_{\text{obs}} = 660$ nm. (●, ■) correspond to the experimental data and the theoretical fit is the dashed line.

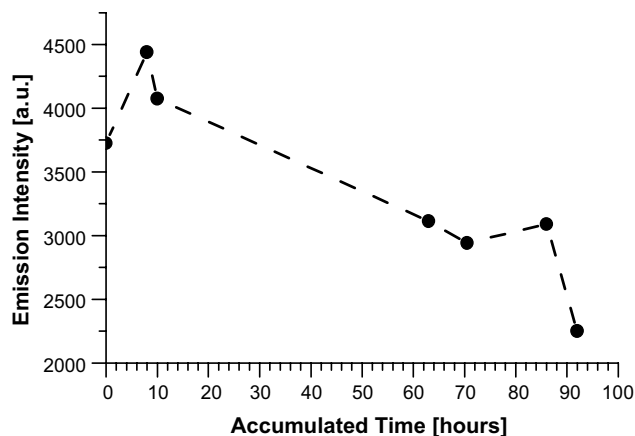


Fig. 5. Evolution of the emission from R6G ORMOSIL kept in the darkness, after the sample was irradiated for 6 h.

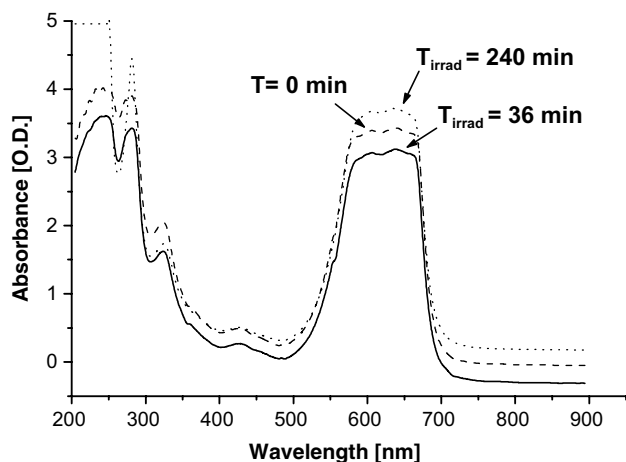


Fig. 6. Absorption spectra of the Nile blue ORMOSIL as function of the time of irradiation.

3.2. Nile blue ORMOSIL

Fig. 6 shows the absorption spectra of the Nile blue ORMOSIL at three different exposure times of irradiation. The absorption decreased when the ORMOSIL was irradiated for 36 min. Then the absorption increased after an irradiation time of 4 h.

Fig. 7(a) and (b) show the emission and excitation intensities as function of the accumulated irradiation energy, respectively. The experimental data were fitted with exponential curves (dashed line). When NB ORMOSIL was irradiated and the amount of energy increased, the emission and excitation intensities increased until they reached a maximum value and then remained constant.

The NB ORMOSIL was also bleached after 6 h of irradiation and it remained colorless for one day. After, the sample was kept in the darkness to avoid the sunlight, and the evolution of the NB ORMOSIL photoluminescence was followed at different times to detect the recovery of this sample. These results are shown in Fig. 8. The sam-

ple showed a little recovery by 36 min (0.6 h) in the darkness and the emission signal increased, which was lost at the time of 6 h. Surprisingly, the ORMOSIL regained homogeneous coloration by 18 h in the absence of sunlight.

Table 1 includes the parameters from NB and R6G ORMOSILs.

Maya [15] calculated the slope efficiency of R6G silica gels. The silica gel was irradiated with a Nd:YAG laser, which is more energetic than a N₂ laser. The slope of R6G silica gel was calculated taking the two points of the curve.¹ We calculate the slope efficiency from NB and the R6G ORMOSILs using the same expression¹ taking the points 1 and 2. Its value is greater than the R6G silica gel efficiency (see Fig. 9). It is important to notice that the slope of R6G ORMOSIL is always bigger than the slope of R6G silica gel if we chose the point 1 and any other point of the graph. Table 2 includes the values of the slope efficiency for all samples.

4. Discussion

It is well known that the laser dyes have a concentration limit, depending on the specific dye [16]. Taking this into account, our samples have a high dye concentration (1.1×10^{-3} M), which represents a concentration in excess of this limit, inhibiting luminescence (concentration quenching) due to energy migration between the molecules. The molecules must be very close, forming aggregates. Therefore, the quenching concentration exists since the beginning of the exposition. We consider that the UV energy is employed in two processes: the first one is the destruction of some monomers, inhibiting its luminescence and decreasing the emission. The second one is the dissociation of the aggregates or dimers, that gives more monomers than can be excited by light and then produce luminescence, but this can give emission if the concentration is low, or can give any emission if there is concentration quenching.

From Fig. 4(a) we deduce that the R6G molecules are destroyed because the emission decreases exponentially. In Fig. 4(b) we observed a little increase in the excitation followed by a signal decay. The processes explained previously are competing between them. When the ORMOSIL is irradiated, the dye molecules are destroyed (degradation), thus reducing their concentration; but the dissociation of aggregates is produced and more monomers become present, increasing the excitation, given no luminescence due to quenching, up to a point where there is no quenching because the concentration is low and there are no more aggregates. At this point excitation reaches its maximum value. After that, the irradiation destroys the single molecules and the emission and excitation signals decays exponentially [17].

¹ The slope was calculated using the next expression: $m = \frac{y_2 - y_1}{x_2 - x_1}$.

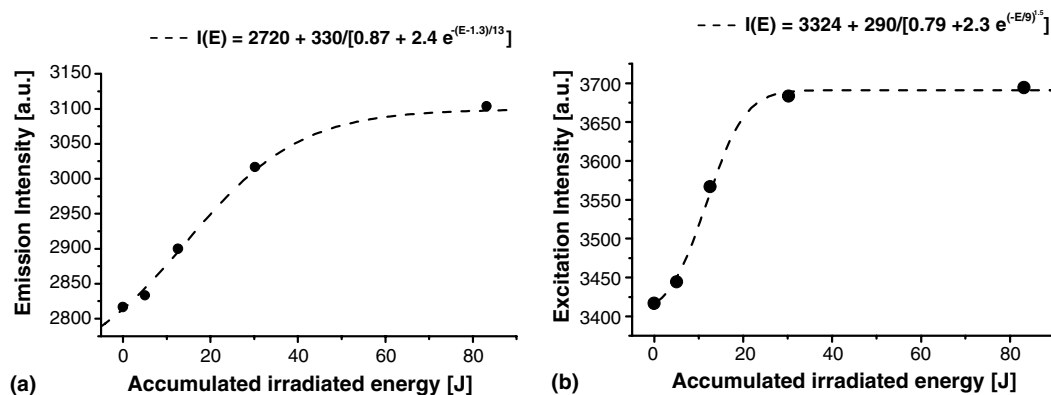


Fig. 7. (a) Emission intensity NB ORMOSIL as function of accumulated irradiated energy with $\lambda_{\text{exc}} = 560$ nm. (b) Excitation intensity of NB ORMOSIL as function of accumulated irradiated energy with $\lambda_{\text{obs}} = 710$ nm. Dots (●) correspond to the experimental data. The theoretical fit is the dashed line.

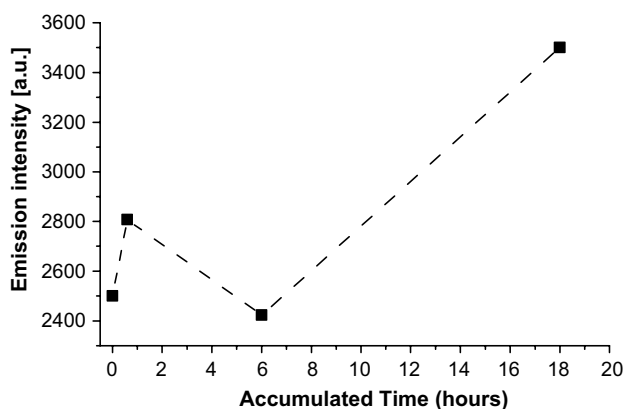


Fig. 8. Evolution of the recovery of the Nile blue ORMOSIL kept in the darkness. Emission intensity was measured at different times after the sample was kept in the darkness.

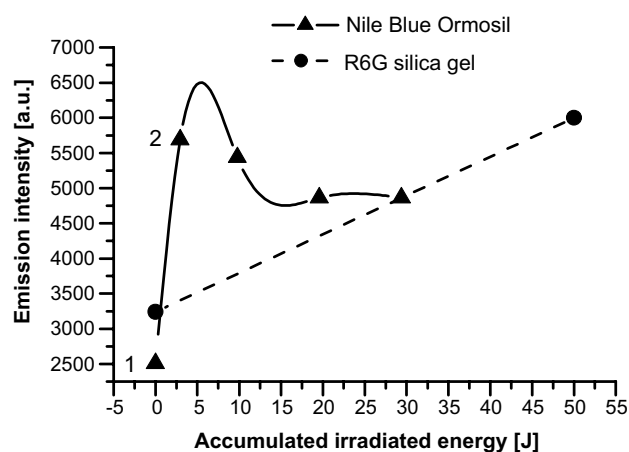


Fig. 9. Emission intensity from R6G silica gel and Nile blue ORMOSIL.

Table 1

Fitting parameters

Figures	Graph	Y_0	A_1	B	C	t_1
4(a)	R6Gemi ^a	32,622	2376	–	–	1.9
4(b)	R6Gexc ^a	17,771	7329.3	–	–	251
7(a)	NBemi ^b	3324	290	0.79	2.3	9
7(b)	NBexc ^b	2720	330	0.87	2.4	13

^a Fit: $Y = Y_0 + A_1 e^{-(x-x_0)/t_1}$.

^b Fit: $Y = Y_0 + A_1 / [B + C e^{-(x-x_0)/t_1}]$.

From Fig. 7, an opposite effect in the NB emission signal was detected in comparison to the R6G ORMOSIL. The excitation signal increases until it reaches a constant value. The NB molecules are very resistant because they absorb less UV energy and the concentration quenching is not acting. The UV energy is being employed in the dissociation of aggregates, which produces more monomers. These monomers absorb and emit until equilibrium is reached.

The normalized photostability is defined as the accumulated pump energy absorbed by the system per mole of dye molecules before the output energy falls to one half of its initial value [8].

Table 2

Calculated slope efficiency

Sample	Slope efficiency (J^{-1})
R6G silica gel	55.2
R6G ORMOSIL	301.3
Nile blue ORMOSIL	1081.6

$$\text{Normalized photostability} = \frac{E_{\text{pulse}} N_{1/2}}{\pi \times r^2 \times l \times C}$$

where E_{pulse} is the pulse energy (in joules), $N_{1/2}$ is the number of pulses to get the half of the initial emission intensity, r is the radius of the laser beam on the surface of the sample and l is the sample thickness (in centimeters) and C is the dye concentration (molar per liter). The units are J/mol . For the R6G ORMOSIL, the consuming pump energy in general is 10 mJ/pulse, the radius on incident laser beam is 0.5 mm, the sample thickness is 7 mm, and the concentration is 1.1×10^{-3} M. Then, the normalized photostability is 1.65 GJ/mol. The organic molecules absorb this energy and it is enough to bring out the bond breaking of the R6G. The NB molecules do not absorb this energy

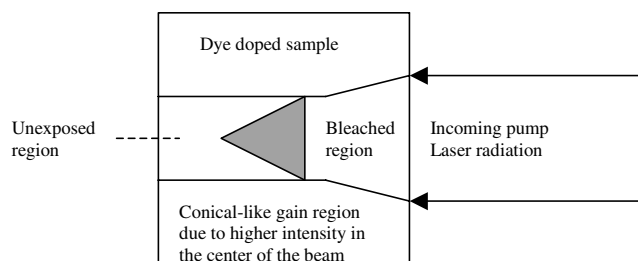


Fig. 10. Scheme of the pump-laser radiation moving through the dye doped sample as photodegradation occurs.

showing a high strength, and a good stability within the ORMOSIL matrix.

The photobleaching effect in both ORMOSILs is examined. The effect of photobleaching in the Rhodamine 6G ORMOSIL (Fig. 5) can be explained in the following way: after irradiation, the bleached area on the surface of the samples is as big as the cross-section area of incident laser beam. As shown in Fig. 10, the laser beam cannot irradiate the entire surface of the sample. Even in the incoming direction of the laser, not all dye molecules are irradiated. The laser energy declines with the incoming depth. So the high energy coming from the laser is shared by only a small part of dyes and organic modifiers in the matrix.

The photobleaching effect in NB ORMOSILs is less notorious (Fig. 8). The ORMOSIL matrix protects the NB molecules of the laser radiation. The ORMOSIL has a continuous porosity and it allows the NB molecules to move from the pores of the irradiated area to the pores of the normal state causing empty pores in the focused part by laser beam. During the absence of sunlight, the NB molecules migrate to the emptied pores, so homogeneous coloration is obtained in the samples. Then, the NB molecules are very stable in the ORMOSIL matrix [18].

Other important factor to improve the photostability is the host matrix and its microstructure. The mixture of TMOS, water, nitric acid, methanol and formamide forms our ORMOSIL matrix. The microstructure of the NB ORMOSIL host is more condensed with small pores. This property limits the mobility of the NB molecules, which decreases the possibility of the photochemical reactions between the dye molecules and other impurities and increases the dye caging. Then, the photodegradation of the NB molecules decreases. For R6G ORMOSIL, the microstructure of the host is not homogeneous and it has a distribution of large pores. This kind of microstructure allows a large mobility of the dye molecules producing optical loss, thermal accumulation and photochemical reactions with impurities. Other important factor is the ester group of the R6G molecule. This group can react with the methanol under acidic conditions (in presence of nitric acid), which does not allow the dye molecules attach to the formamide SiO₂ network. Under these conditions, the degradation of the R6G molecules is very possible within the ORMOSIL.

Finally, Fig. 9 shows that the Nile blue and Rhodamine 6G molecules incorporated in the ORMOSIL matrix have a higher efficiency than the R6G silica gel. It proves that the ORMOSIL matrix is an excellent host to protect the dye molecules of the laser radiation, and it improves the photostability of the dye molecules.

5. Conclusions

The sol-gel process offers an opportunity to incorporate organic molecules into ORMOSIL matrices, enhancing their optical properties such as their efficiency and photostability in comparison to silica gels prepared by the same process.

The photochemical reactions such as dimerization of the dye molecules and the structural variations of the solid matrix ORMOSILs under laser irradiation can be detected by spectroscopy techniques. Both define the photostability of the dye molecules into the matrix ORMOSIL.

The degradation of the organic molecules produces an exponential decay. The increase of the signal is due to the molecules activation and the caging of the dye by the matrix ORMOSIL that avoid the interactions with other species. The homogeneous microstructure with small pores offers a more stable matrix, caging the dye molecules and improving their photostability. The NB ORMOSIL offers a more stable matrix than the R6G ORMOSIL.

Although the normalized photostability from NB ORMOSIL is the same as the R6G ORMOSIL, it is clear that the quenching of the luminescence was not produced due to the photostability of the NB molecules in the ORMOSIL matrix.

Acknowledgements

The author gratefully acknowledges the financial support for this work from the UCMEXUS, DGAPA-UNAM IN11902 and ECOS M02-P02. The author thanks to Dr. J. Garcia M. for his valuable commentaries to this work.

References

- [1] X. Li, T.A. King, *J. Non-Cryst. Solids* 204 (1996) 235.
- [2] B. Lintner, N. Arfsten, H. Dislich, *J. Non-Cryst. Solids* 100 (1988) 378.
- [3] L.M. Sheppard, *Ceram. Bull.* 67 (11) (1988) 1179.
- [4] J.Y. Tseng, C.-Y. Li, T. Takada, C. Lechner, J.D. Mackenzie, *SPIE* 1758 (1992) 612.
- [5] J. Hect, *Laser Focus World* 28 (7) (1992) 59.
- [6] F.P. Schafer, *Dye Lasers*, third ed., Springer Verlag, New York, 1990.
- [7] J.C. Altman, R.E. Stone, *SPIE* 1758 (1992) 507.
- [8] Y. Yang, M. Wang, G. Qian, Z. Wang, X. Fan, *Opt. Mater.* 24 (2004) 621.
- [9] T. Suratwala, Z. Gardlund, K. Davidson, D.R. Uhlmann, *J. Sol-Gel Sci. Technol.* 8 (1997) 953.
- [10] J. Kosar, *Light-Sensitive Systems*, Wiley, New York, 1965.
- [11] I.P. Kamirov, L.W. Stulz, E.A. Chandross, C.A. Pryde, *Appl. Opt.* 11 (7) (1972) 1563.
- [12] Y. Zhang, M. Wang, Z. Wang, G. Qian, *Mater. Lett.* 40 (1999) 175.

- [13] D. Avnir, V. Kaufman, R.J. Reisfeld, *J. Non-Cryst. Solids* 74 (1985) 395.
- [14] J. McKiernan, S. Yamanaka, B. Dunn, J.I. Zink, *J. Phys. Chem.* 94 (1990) 5652.
- [15] O. Maya Padilla. “Fotodegradación de la Rodamina 6G y luminescencia del Eu^{2+} en geles de SiO_2 ”. Thesis, UNAM, 1998.
- [16] J. Garcia, M.E. Ramírez, M.A. Mondragón, *J. Sol–Gel Sci. Technol.* 13 (1998) 657.
- [17] J. Rickards, J. Garcia, M.R. Garcia, M.E. Ramírez, K. Lopez, *Nucl. Instr. Meth. Phys. Res. B* 127 (1997) 691.
- [18] A. Parvathy Rao, A. Venkateswara Rao, *Sci. Technol, Adv. Mater.* 2 (2003) 121.